

Scaling regimes and functional renormalization for wetting transitions

Reinhard Lipowsky* and Michael E. Fisher

Baker Laboratory, Cornell University, Ithaca, New York 14853

(Received 12 January 1987)

Interface unbinding transitions, such as those arising in wetting phenomena, are studied in d dimensions with general interactions. Three scaling regimes must be distinguished: a mean-field (MF), a weak-fluctuation (WFL), and a strong-fluctuation (SFL) regime. A simple picture clarifies the origin and nature of the different regimes and correctly describes the MF and WFL critical behavior. In the SFL regime, however, this picture fails, as do more elaborate perturbative methods. To overcome this an approximate functional renormalization group is introduced: it acts as a nonlinear map in the space of interaction potentials, $V(l)$, for two interfaces at a separation l . The formulation is exact to first order in V and embodies the correct scaling behavior at a continuous unbinding transition. In the SFL regime, it reveals two nontrivial fixed point potentials, $V_0^*(l)$ and $V_c^*(l)$, which describe, respectively, the completely delocalized phase and the critical manifold for the unbinding transition. On approaching the upper boundary dimension, $d_u=3$, these fixed points do not coalesce with the standard Gaussian fixed point but, rather, mutually annihilate leaving a line of novel "drifting" fixed points. For $d < 3$, sufficiently long-ranged perturbations cause crossover to the WFL and MF regimes. Thus the functional renormalization-group approach yields a unified description of all scaling regimes.

I. INTRODUCTION

In many situations, the behavior of an interface (or domain wall or membrane) is constrained by external fields or by the presence of other interfaces. These external constraints usually tend to localize the interface. On the other hand, thermal fluctuations or fluctuations induced by quenched impurities lead to an interfacial wandering which competes with this localization. As a result, the interface may undergo an unbinding (or delocalization or depinning) transition where it transforms from a localized to a delocalized state.

Various classes of unbinding phenomena can be distinguished: (a) the delocalization of a *single* interface in an external potential. An example is the roughening transition;¹ (b) the unbinding of *two* interacting interfaces: this is the mechanism behind the critical effects at wetting;²⁻⁴ (c) the unbinding of an assembly of interfaces which occurs at commensurate-incommensurate transitions⁴ and during the swelling of lyotropic liquid crystals.⁵

This paper mainly concerns the unbinding of two interfaces. First, we discuss the construction of effective interfacial models. Then, a simple picture is presented in Sec. III which shows that unbinding transitions can exhibit three different scaling regimes depending on the spatial dimensionality, d , and on the character of the microscopic interactions:⁶⁻⁸ (i) a mean-field (MF) regime for large d and/or sufficiently long-ranged interactions; (ii) a weak-fluctuation (WFL) regime with nonclassical exponents but the same (trivially determined) phase boundaries as in MF theory; (iii) a strong-fluctuation (SFL) regime in which both exponents and phase boundaries are nontrivial. The critical behavior in the MF and in the WFL regime is correctly given within the simple picture as can be demon-

strated by more elaborate perturbative arguments. However, in the SFL regime, both the simple picture and the perturbative methods are not applicable. As described briefly in a previous communication,⁹ we have introduced and applied a nonlinear functional renormalization group (RG) in order to study this nontrivial regime. This RG approach, which is an extension of Wilson's approximate integral recursion relation,¹⁰ is described in Sec. IV. It is *exact* to linear order in the effective Hamiltonian. Some useful bounds on the behavior implied by these recursion relations are obtained in Sec. V. The numerical results obtained from this functional RG for short-range interactions are described in detail in Sec. VI. Two distinct nontrivial fixed points are found for interfaces subject only to thermal fluctuations. These fixed points bifurcate in an unusual way⁹ from a line of "drifting" fixed points at the upper borderline dimension $d=3$ rather than from the Gaussian fixed point as normally expected. The two fixed points describe the critical manifold and the completely delocalized phase, respectively. Long-range perturbations are considered briefly in Sec. VI D. Finally, Sec. VII contains a summary and a discussion of our results.

II. INTERFACE MODELS

In this section, we will discuss effective models which describe the fluctuations and interactions of two interfaces or domain walls. We motivate these models by reference to wetting phenomena.²⁻⁴ However, similar models can also be used to discuss different phenomena such as commensurate-incommensurate transitions and the swelling of lyotropic liquid crystals.^{4,5,11}

Interfacial wetting phenomena arise in systems where three distinct thermodynamic phases, α , β , and γ can coexist. In such systems, the $\alpha\gamma$ interface may contain, in

thermal equilibrium, a layer of the β phase, see Fig. 1(a). We will assume here that the system is not close to any bulk critical point. Therefore, the thermal fluctuations *within the bulk phases* α , β , and γ are governed by microscopic length scales. On the other hand, the thermal fluctuations can be correlated over a much wider range *within the interfacial regions*. Then, the interfacial correlation length, see (3.15) below, increases with increasing thickness of the intermediate β layer. This happens if the temperature, T , is above the roughening temperature, T_R , for one of the interfaces bounding the layer.

Each interface will have its own roughening temperature. We will focus on the case in which the $\alpha\beta$ interface is rough while the $\beta\gamma$ interface is smooth, see Fig. 1(b). Thus, we will in effect study a fluctuating $\alpha\beta$ interface in the presence of a rigid wall which may represent a solid surface. Our results do apply, however, equally well to the case where both interfaces bounding the β layer are rough. The equivalence of these two situations has been shown previously.^{12,13,3} If both interfaces are smooth, i.e., $T < T_R^{\alpha\beta}$ and $T < T_R^{\beta\gamma}$, the correlations in the interfacial region will *not* grow significantly above those in the bulk phases. This situation which occurs, for example, for multilayering² and commensurate-incommensurate transitions, is not considered here (but see, e.g., Ref. 11).

To proceed, let \mathbf{x} be the longitudinal coordinate (x_1, \dots, x_{d-1}) and z be the coordinate perpendicular to the wall, and call the fluctuating distance of the $\alpha\beta$ interface from the $\beta\gamma$ plane $l(\mathbf{x})$; see Fig. 1(b). The free-energy functional or effective Hamiltonian for the interfacial configurations is then taken to be

$$\mathcal{H}\{l\} = \int d^{d-1}x \left[\frac{1}{2} \bar{\Sigma}(\nabla l)^2 + V_W(l) \right] / k_B T. \quad (2.1)$$

The first term represents the *elastic* free energy of the $\alpha\beta$ interface, the second term the direct *interaction* free energy of the interface with the wall. The model (2.1) implicitly contains a small-scale, spatial cutoff, $1/\Lambda$, which is of the order of the intrinsic width of the interface, i.e., of the order of the bulk correlation lengths.

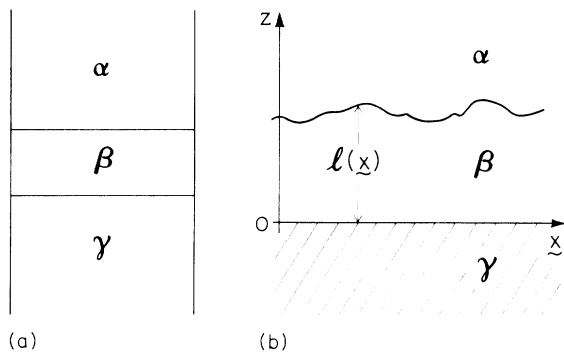


FIG. 1. (a) A prewetting layer, β , intruding between two bulk phases α and γ and bounded by two interfaces $\alpha\beta$ and $\beta\gamma$. (b) Specification of the $\alpha\beta$ interface by its separation, $l(\mathbf{x})$, from a rigid-wall interface, $\beta\gamma$.

A. Elastic free energy

The elastic free energy controls the interfacial fluctuations when the interface is “free,” i.e., completely separated from the wall. The parameter $\bar{\Sigma}$ in (2.1) is the interfacial *stiffness*. If both α and β are fluid phases, the interfacial *tension*, Σ , is isotropic and $\bar{\Sigma} = \Sigma$. If α and/or β are solid phases, the tension is anisotropic, i.e., $\Sigma = \Sigma(\hat{\mathbf{n}})$ where $\hat{\mathbf{n}}$ is the unit vector normal to the $\alpha\beta$ interface. Quite generally, $\Sigma(\hat{\mathbf{n}})$ attains a local minimum, say Σ_0 , for $\hat{\mathbf{n}}$ parallel to a lattice axis. Here, this axis is taken to be the z axis; see Fig. 1(b). Since we assume that the $\alpha\beta$ interface is rough, the tension Σ is a smooth function in the vicinity of this minimum. If $\Sigma(\hat{\mathbf{n}})$ does not depend strongly on the azimuthal orientation of $\hat{\mathbf{n}}$, the stiffness in (2.1) is given by^{14–16} $\bar{\Sigma} = \Sigma_0 + (d^2\Sigma/d\theta^2)_0$, where θ is the angle between the z axis and the normal. If $\Sigma(\hat{\mathbf{n}})$ depends on the azimuthal orientation, one should replace $\bar{\Sigma}(\nabla l)^2$ in (2.1) by the tensorial expression $(\partial l/\partial x_\alpha) \bar{\Sigma}_{\alpha\beta} (\partial l/\partial x_\beta)$, where $\bar{\Sigma}_{\alpha\beta}$ is a symmetric tensor.

Strictly speaking, the stiffness $\bar{\Sigma}$ which enters in (2.1) depends on the length scale of the interfacial fluctuations. For excitations on molecular scales, this parameter is determined by microscopic intermolecular forces. In the long-wavelength limit, on the other hand, $\bar{\Sigma}$ is given in terms of the interfacial tension Σ of a planar interface. This macroscopic stiffness is infinite for temperatures below the roughening temperature, T_R , and zero at the critical temperature, T_c . As mentioned, we are concerned here with the temperature range $T_R < T < T_c$ which implies that the long-wavelength limit of the stiffness is finite. In this case, the scale-dependent part of $\bar{\Sigma}$ is a correction term and will not affect the interfacial critical behavior described below.

B. Interaction free energy

The interaction free energy, per unit area, of the interface with the wall is described by $V_W(l)$ in (2.1). *Near* the $\alpha\beta$ phase boundary, it has the generic form

$$V_W(l) = Hl + V(l), \quad (2.2)$$

with $V(l) \rightarrow 0$ for $l \rightarrow \infty$. The variable H measures the distance from the $\alpha\beta$ phase boundary. In a fluid context, H is typically a chemical potential difference, $\delta\mu$, measuring departure from bulk coexistence. At $\alpha\beta$ phase coexistence with $H=0$, the interaction is given by $V(l)$ alone. In general, $V(l)$ may have several minima. Here, we will focus on the situation where $V(l)$ achieves a single minimum at finite or infinite l . This form is appropriate for the purpose of discussing phase transitions in which the interface *unbinds continuously* from the wall.

To describe wetting phenomena, the precise form of $V(l)$ depends on the microscopic forces between the particles in the α , β , and γ phases. Let us assume, for instance, that α and β are both fluid phases while γ is a solid phase. Then, we can distinguish between fluid-fluid and solid-fluid interactions. If both types of microscopic interactions decay at least exponentially for large separations between the molecules, one has^{17,18}

$$V(l) \approx -W \exp(-ml/\xi_\infty) + U \exp(-nl/\xi_\infty), \quad (2.3)$$

for large l , where m and n are two dimensionless constants with $n > m$. The parameter ξ_∞ is the correlation length within the β layer. The amplitude W will be regarded as a basic "control" parameter or thermodynamic field varying, typically, through zero as the temperature, T , and/or a short-ranged surface field increases. If (i) the microscopic interactions decay faster than exponentially, one has $(m,n)=(1,2)$ for *critical* unbinding transitions. These values for m and n also apply if (ii) the microscopic fluid-fluid and solid-fluid interactions decay exponentially and the range, R_0 , of the solid-fluid interaction satisfies $R_0 < \frac{1}{2}\xi_\infty$. For (iii) $\xi_\infty > R_0 > \frac{1}{2}\xi_\infty$, on the other hand,¹⁹ one has $(m,n)=(1,\xi_\infty/R_0)$. For *tricritical* and *tetracritical* unbinding transitions, one has, for case (i), $(m,n)=(1,3)$ and $(m,n)=(1,4)$, respectively.¹⁷

If the molecules interact through power-law forces, the interaction $V(l)$ has the general form^{6,20-24}

$$V(l) \approx -W/l^r + U/l^s, \quad s > r. \quad (2.4)$$

Again, W is regarded as a basic thermodynamic field passing through zero as the temperature or a surface field varies. If both solid-fluid and fluid-fluid interactions vary as $1/R^{d+\sigma}$ for large separations R between the molecules, one finds^{6,23,24} $(r,s)=(\sigma-1,\sigma)$, $(\sigma-1,\sigma+1)$, and $(\sigma-1,\sigma+2)$ for critical, tricritical, and tetracritical transitions. Finally, one may also consider the interaction

$$V(l) \approx -W/l^r + U \exp(-l/\xi_\infty), \quad (2.5)$$

which would be appropriate for short-range fluid-fluid and long-range solid-fluid forces.^{25,26}

Strictly speaking, the above expressions, (2.3)–(2.5), for $V(l)$ represent the asymptotic behavior for large l . For small l , i.e., near the wall, $V(l)$ will, in general, have some different l dependence. Near a solid wall, for instance, $V(l)$ is expected to contain oscillations on a scale which is set by the size of the molecules.²⁷ However, since we are interested in the critical behavior when \bar{l} , the mean distance of the interface from the wall, is large, we will ignore the details of $V(l)$ for small l and will accept the above expressions for all *positive* values of l .

Negative values of l are, in fact, unphysical since l is a distance. Thus, for consistency, one should supplement the interface potentials $V(l)$ by the *hard* wall condition

$$V(l) = \infty \quad \text{for } l < 0. \quad (2.6)$$

Such a wall is, however, difficult to treat in a perturbative way. Furthermore, one might expect that the precise nature of the wall will not affect the critical behavior at the unbinding transition. Therefore, two other types of walls have been considered: (i) a *soft* wall,¹⁷ i.e.,

$$V(l) \rightarrow \infty \quad \text{as } l \rightarrow -\infty, \quad (2.7)$$

and (ii) a *finite* wall⁷ given by

$$V(l) = c \quad \text{for } l < 0, \quad (2.8)$$

with c a positive constant.

III. CONTINUOUS UNBINDING TRANSITIONS: SIMPLE PICTURE

Quite generally, the interface potentials as given by (2.3)–(2.5) consist of an *attractive* part which favors a

small value of l and a *repulsive* part which favors a large value. For $W > 0$ and $W \leq 0$, the potentials have a minimum at finite and infinite l , respectively; see Fig. 2. By varying W , one can change from a net attractive to a net repulsive regime. A *continuous unbinding transition* occurs when W approaches, from above, a critical value W_c . For $W > W_c$, the attractive part is strong enough to bind the interface to the wall. For $W \leq W_c$, on the other hand, the interface is completely separated from the wall.

For fixed interaction, $V(l)$, three different scaling regimes have to be distinguished: (a) a mean-field (MF) regime for $d > d_1$; (b) a weak fluctuation (WFL) regime for $d_1 > d > d_2$; (c) a strong-fluctuation (SFL) regime for $d < d_2$. The borderline dimensionalities d_1 and d_2 depend on the form of $V(l)$. In this section, we show that these dimensionalities can be obtained, quite generally, within a simple heuristic picture.^{8,3,4}

A. Free interface

First, let us consider the case $W \leq W_c$ when the interface is completely separated from the wall. Such an interface is controlled by the effective Hamiltonian

$$\mathcal{H}_0\{l\} = \int d^{d-1}x \frac{1}{2} \bar{\Sigma} (\nabla l)^2, \quad (3.1)$$

which should be compared with (2.1). The interfacial configurations can be characterized by the difference correlation function defined by

$$\begin{aligned} \Delta C(x) &\equiv \frac{1}{2} \langle [l(\mathbf{x}) - l(\mathbf{0})]^2 \rangle \\ &= \frac{k_B T}{\bar{\Sigma}} \int \frac{d^{d-1}p}{(2\pi)^{d-1}} \frac{1 - e^{i\mathbf{p} \cdot \mathbf{x}}}{p^2}, \end{aligned} \quad (3.2)$$

in which the momentum integration extends up to a cutoff $|\mathbf{p}| = \Lambda$. The behavior of $\Delta C(x)$ for large x depends on the dimensionality. For $d > 3$, one finds

$$\Delta C(x) \approx \frac{k_B T}{\bar{\Sigma}} \Omega_0 / \Lambda^{3-d} \quad (3.3)$$

for large x , with the nonuniversal coefficient

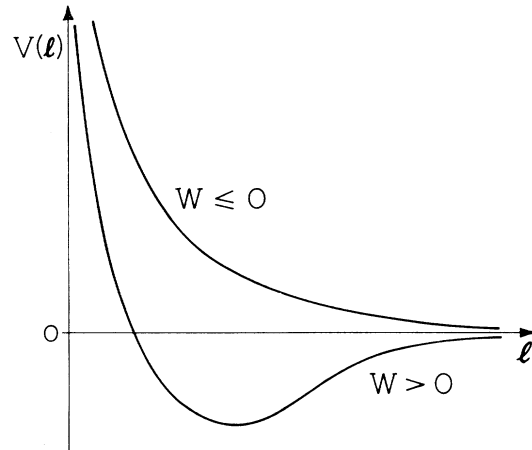


FIG. 2. Typical interfacial potentials for positive and negative values of the parameter W .

$$\Omega_0 \simeq (2\pi)^{(1-d)/2} / 2^{(d-3)/2} (d-3) \Gamma(\frac{1}{2}d - \frac{1}{2}), \quad (3.4)$$

which depends on the details of the cutoff. Clearly $\Delta C(\infty)$ also depends directly on the momentum cutoff. For $d=3$, one has

$$\Delta C(x) = \frac{k_B T}{\bar{\Sigma}} \frac{1}{2\pi} \ln(\Lambda x) + O(1), \quad (3.5)$$

while, for $d < 3$, one obtains

$$\Delta C(x) = \frac{k_B T}{\bar{\Sigma}} \Psi_0 |x|^{3-d} + O(1), \quad (3.6)$$

with the universal coefficient

$$\Psi_0 = |\Omega_0| = \frac{1}{2} \pi^{(1-d)/2} \Gamma\left(\frac{d-1}{2}\right) / (3-d), \quad (3.7)$$

which is cutoff-independent. Thus, a free interface subject only to thermally-induced fluctuations has a borderline dimensionality

$$d_0 = 3. \quad (3.8)$$

Now, an interfacial segment of longitudinal dimension L_{\parallel} has, on average, a transverse dimension

$$L_{\perp} \equiv [\Delta C(L_{\parallel})]^{1/2}. \quad (3.9)$$

Using (3.3)–(3.7), this relation leads to

$$L_{\perp} \approx [(k_B T / \bar{\Sigma}) \Omega_0]^{1/2} / \Lambda^{\zeta} \quad \text{for } d > 3, \quad (3.10)$$

$$\approx [(k_B T / 2\pi \bar{\Sigma}) \ln(\Lambda L_{\parallel})]^{1/2} \quad \text{for } d = 3, \quad (3.11)$$

and finally,

$$L_{\perp} \approx [(k_B T / \bar{\Sigma}) \Psi_0]^{1/2} L_{\parallel}^{\zeta} \quad \text{for } d < 3, \quad (3.12)$$

for L_{\parallel} large compared to $1/\Lambda$ where we have defined a *spatial anisotropy or roughness exponent*^{4,8}

$$\zeta \equiv \frac{1}{2}(3-d). \quad (3.13)$$

Thus, the typical fluctuations which might be pictured as ‘‘humps’’ of an interfacial segment with longitudinal dimension L_{\parallel} , are characterized by a transverse dimension $L_{\perp} \ll L_{\parallel}$ for $d > 1$.

B. Anisotropic scaling

Now, consider an interface whose mean distance \bar{l} from the wall is large but finite. In this case, its fluctuations are governed by two length scales, ξ_{\parallel} and ξ_{\perp} . For large x , the correlation function

$$C(x) \equiv \langle [l(x) - \bar{l}][l(0) - \bar{l}] \rangle \quad (3.14)$$

will decay in directions parallel to the interface as

$$C(x) \sim \exp(-x/\xi_{\parallel}), \quad (3.15)$$

where ξ_{\parallel} is the *longitudinal correlation length*. This exponential behavior has been found both within Ornstein-Zernike theory^{3,28} and from exact calculations in $d=2$.³ These calculations also show that the interfacial *roughness*,

$$\xi_{\perp} \equiv [\langle (l - \bar{l})^2 \rangle]^{1/2} = \sqrt{C(0)}, \quad (3.16)$$

is finite for a bound interface as one would expect. Note that ξ_{\perp} is related to the difference correlation function

$$\Delta C(x) = \frac{1}{2} \langle [l(0) - l(x)]^2 \rangle, \quad (3.17)$$

via

$$\Delta C(\infty) = \xi_{\perp}^2. \quad (3.18)$$

It is natural to assume that, for ξ_{\parallel} finite, $\Delta C(x)$ has a scaling form $\Delta C(x) \approx \xi_{\parallel}^{y_1} \Psi(x/\xi_{\parallel})$ with, say, $\Psi(z) \sim z^{y_2}$ for $z \rightarrow \infty$. At the transition point, i.e., for $\xi_{\parallel} \rightarrow \infty$, one must recover the behavior for the free interface. This implies $y_1 = y_2 = 2\zeta$ with ζ given by (3.13). Thus, for $d < d_0 = 3$, the difference correlation function should assume the scaling form

$$\Delta C(x) \approx (k_B T / \bar{\Sigma}) \xi_{\parallel}^{2\zeta} \Psi(x/\xi_{\parallel}), \quad (3.19)$$

with

$$\Psi(z) \approx \Psi_0 z^{2\zeta} \quad \text{for } z \rightarrow 0, \quad (3.20)$$

where Ψ_0 is given by (3.7). This scaling behavior is fully confirmed by exact calculations for $d=2$.³ For the marginal case $d = d_0 = 3$, scaling arguments lead to

$$\Delta C(x) = \frac{k_B T}{2\pi \bar{\Sigma}} \ln[\Lambda \xi_{\parallel} \Phi(x/\xi_{\parallel})], \quad (3.21)$$

with

$$\Phi(z) \approx z \quad \text{for } z \rightarrow 0. \quad (3.22)$$

From (3.18)–(3.22), the interfacial roughness follows as

$$\xi_{\perp} \approx [(k_B T / \bar{\Sigma}) \Psi_{\infty}]^{1/2} \xi_{\parallel}^{\zeta} \quad \text{for } d < d_0, \quad (3.23)$$

$$\approx [(k_B T / 2\pi \bar{\Sigma}) \ln(\Lambda \xi_{\parallel})]^{1/2} \quad \text{for } d = d_0, \quad (3.24)$$

when ξ_{\parallel} is large. Note that the coefficient Ψ_{∞} is, in general, not equal to Ψ_0 as given by (3.7). Finally, for $d > d_0$, the typical amplitude for the long-wavelength excitations depends on the microscopic cutoff Λ . From (3.10), one finds

$$\xi_{\perp} \approx [(k_B T / \bar{\Sigma}) \Omega_0]^{1/2} / \Lambda^{\zeta}, \quad d > d_0. \quad (3.25)$$

In summary, the typical configurations of an interface which is bound to the wall consist of large excursions with longitudinal and transverse dimension ξ_{\parallel} and ξ_{\perp} . These humps are thus essentially confined between $z \simeq \bar{l} - \xi_{\perp}$ and $z \simeq \bar{l} + \xi_{\perp}$, see Fig. 3. As we will see, one has either $\bar{l} \gg \xi_{\perp}$ or $\bar{l} \simeq \xi_{\perp}$.

C. Effective interactions

Now, we attempt to estimate the difference between the free energy of a bound and a free interface. This free-energy difference consists of three parts: (i) an energy change resulting from the interaction with the wall which we divide into an attractive part $V_A(l) \leq 0$ and a repulsive part $V_R(l) \geq 0$:

$$V(\bar{l}) = V_A(\bar{l}) + V_R(\bar{l}); \quad (3.26)$$

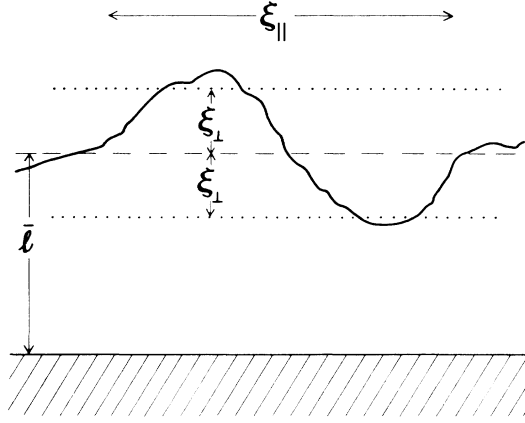


FIG. 3. Illustration of a typical interfacial fluctuation showing the mean thickness, \bar{l} , and the longitudinal and transverse correlation lengths, ξ_{\parallel} and ξ_{\perp} , respectively.

(ii) the increase in the bending energy;⁸ (iii) an overall loss of entropy resulting from the confinement of the interfacial fluctuations,¹⁵ see Fig. 3.

The increase Δe , in the bending energy per unit area arises from the gradient term in the effective Hamiltonian (2.1). For humps with longitudinal and transverse dimensions ξ_{\parallel} and ξ_{\perp} , this increase can be estimated from (2.1) as

$$\Delta e \simeq \bar{\Sigma} (\xi_{\perp} / \xi_{\parallel})^2. \quad (3.27)$$

Similarly, the loss of entropy per unit area, Δs , can be estimated if we imagine putting rigid walls at $z \simeq \bar{l} - \xi_{\perp}$ and $z \simeq \bar{l} + \xi_{\perp}$. Then, each collision of the interface with these confining walls leads to an entropy loss of order k_B .¹⁵ Furthermore, the density of collisions is of order $1/\xi_{\parallel}^{d-1}$. Therefore, we obtain

$$\Delta s \simeq -k_B / \xi_{\parallel}^{d-1}. \quad (3.28)$$

Thus, the total change in free energy per unit area, Δf , of the interface resulting from the interaction with the wall can be written as

$$\Delta f = V_A(\bar{l}) + V_R(\bar{l}) + U_{\text{FL}}(\xi_{\parallel}), \quad (3.29)$$

with a fluctuation-induced part

$$U_{\text{FL}}(\xi_{\parallel}) = \Delta e - T\Delta s, \quad (3.30)$$

which on using (3.23)–(3.25) becomes

$$U_{\text{FL}}(\xi_{\parallel}) \simeq k_B T (1/\Lambda^{2\xi} \xi_{\parallel}^2 + 1/\xi_{\parallel}^{d-1}), \quad d > d_0 \quad (3.31)$$

$$\simeq k_B T [(2\pi)^{-1} \ln(\Lambda \xi_{\parallel}) + 1] / \xi_{\parallel}^2, \quad d = d_0 \quad (3.32)$$

$$\simeq k_B T / \xi_{\parallel}^{d-1}, \quad d < d_0 \quad (3.33)$$

with $d_0 = 3$. In (3.33), we have used the fact that, for $d < d_0$, both the bending energy and the entropy loss give a contribution of the same order since (3.23) implies

$$\bar{\Sigma} (\xi_{\perp} / \xi_{\parallel})^2 \simeq k_B T / \xi_{\parallel}^{d-1}, \quad \text{for } d < d_0. \quad (3.34)$$

This property is special to thermally-induced fluctuations of the interface as studied here. It does *not* hold for inter-

faces in systems with quenched impurities where the increase in bending energy has a more singular behavior as $\xi_{\parallel} \rightarrow \infty$ than does the entropy loss.⁸

For $d \leq d_0$, it is useful to express ξ_{\parallel} in terms of ξ_{\perp} and to define

$$V_{\text{FL}}(\xi_{\perp}) \equiv U_{\text{FL}}(\xi_{\parallel}(\xi_{\perp})) \quad (d \leq d_0). \quad (3.35)$$

Then, one has

$$V_{\text{FL}}(\xi_{\perp}) \simeq (\bar{\Sigma} \xi_{\perp}^2 + k_B T) \Lambda^2 \exp(-4\pi \xi_{\perp}^2 \bar{\Sigma} / k_B T) \quad (3.36)$$

for $d = d_0$, and

$$V_{\text{FL}}(\xi_{\perp}) \simeq k_B T (k_B T / \bar{\Sigma})^{\tau/2} / \xi_{\perp}^{\tau} \quad (3.37)$$

for $d < d_0$, with a decay exponent

$$\tau \equiv 2(1 - \xi) / \xi = (d - 1) / \xi = 2(d - 1) / (3 - d). \quad (3.38)$$

D. Three scaling regimes

Now, we will determine the equilibrium values of \bar{l} , ξ_{\parallel} , and ξ_{\perp} by minimizing the excess free energy (3.29). First, consider $d > d_0$ where $U_{\text{FL}}(\xi_{\parallel})$ is given by (3.31), and let us assume that the leading contribution to Δf is given by the interaction V . Then, \bar{l} follows from the condition $\partial V(l) / \partial l |_{\bar{l}} = 0$, while ξ_{\parallel} is determined via the curvature from²⁶ $\bar{\Sigma} / \xi_{\parallel}^2 = d^2 V / dl^2 |_{\bar{l}}$ as in standard MF theory for bulk critical phenomena. If this expression for ξ_{\parallel} is inserted into (3.31), one finds that $U_{\text{FL}}(\xi_{\parallel})$ is indeed a correction term as assumed. In fact, $U_{\text{FL}}(\xi_{\parallel})$ as given by (3.31) can be obtained in a more systematic way from the one-loop contribution to the free energy.

Next, consider $d \leq 3$, and the expression

$$\Delta f = V_A(\bar{l}) + V_R(\bar{l}) + V_{\text{FL}}(\xi_{\perp}) \quad (3.39)$$

with V_{FL} given by (3.35)–(3.37). If we postulate $\bar{l} \gg \xi_{\perp}$, we find again that $\Delta f \simeq V_A(\bar{l}) + V_R(\bar{l})$ provided the direct repulsive interaction $V_R(l)$ decays more slowly than the fluctuation-induced repulsion $V_{\text{FL}}(l)$, i.e.,

$$V_{\text{FL}}(l) / V_R(l) \rightarrow 0 \quad \text{as } l \rightarrow \infty. \quad (3.40)$$

In this case, one again recovers the results of MF theory. One can now check that the assumption $\bar{l} \gg \xi_{\perp}$ is self-consistently satisfied by calculating ξ_{\perp} within the Ornstein-Zernike approximation. One indeed finds $\bar{l} \gg \xi_{\perp}$ provided (3.40) is satisfied.

For fixed interaction $V(l)$, the *upper critical dimension* d_1 can be obtained from

$$V_R(l) \sim V_{\text{FL}}(l) \sim 1/l^{\tau(d)} \quad (l \rightarrow \infty), \quad (3.41)$$

where $\tau(d)$ is given by (3.38). This simple criterion is fully confirmed by hyperscaling arguments²⁶ and by a systematic perturbation expansion of the Hamiltonian (1.1) around MF theory.⁶ Thus, for the power law interactions (2.4), d_1 follows from $s = \tau(d_1)$ which yields²⁶

$$d_1 = (3s + 2) / (s + 2). \quad (3.42)$$

On the other hand, if $V_R(l)$ decays faster than any power as in (2.3) and (2.4), one finds²⁶

$$d_1 = d_0 = 3, \quad (3.43)$$

since MF theory is correct for $d > 3$, as mentioned, and one also has $V_{\text{FL}}(l) \gg V_R(l)$ for $d < 3$. The same conclusion follows from (3.42) in the limit $s \rightarrow \infty$, which should correspond to faster than power-law decay.

If the direct and the fluctuation-induced repulsions are equally important—see (3.41)—the roughness, ξ_\perp , as calculated within Ornstein-Zernike theory is of the same order as the mean separation \bar{l} , i.e., $\xi_\perp \sim \bar{l}$ for $\bar{l} \rightarrow \infty$. Since the interfacial fluctuations become more pronounced for lower d , this relation is expected to remain valid for $d < d_1$. The possibility $\xi_\perp \gg \bar{l}$ can be ruled out since the typical excursions are small-amplitude excitations in the sense that $\xi_\perp \ll \xi_\parallel$; see Fig. 3. If $\bar{l} \sim \xi_\perp$ is assumed, minimization of the excess free energy (3.39) leads to the conclusion that the critical behavior is governed by

$$\Delta f \simeq V_A(\bar{l}) + V_{\text{FL}}(\bar{l}) \quad (3.44)$$

provided

$$V_R(l)/V_{\text{FL}}(l) \sim V_{\text{FL}}(l)/V_A(l) \rightarrow 0 \quad (3.45)$$

as $l \rightarrow \infty$. (Note that the case $d = d_0 = 3$ with potentials decaying faster than a power law is excluded here.) In fact, this characterizes the intermediate *weak-fluctuation* (WFL) regime. In this case, the critical behavior can be obtained in a MF fashion if the repulsive interaction $V_R(l)$ is replaced by $V_{\text{FL}}(l)$ in (2.1). One then finds that the critical exponents acquire nonclassical values which depend on τ , as given by (3.38), and thus, on d . However, the *phase boundary* is still given by $W = W_c = 0$ as in the MF regime. Furthermore, the roughness ξ_\perp is found to satisfy $\bar{l} \sim \xi_\perp$ as postulated. The critical exponents determined in this simple way are fully confirmed by (i) a systematic perturbation expansion which can be solved self-consistently up to arbitrary order in $V(l)$,⁶ and (ii) by a linear functional renormalization group which includes terms up to first order in $V(l)$, where $V(l)$ is taken to have a finite wall as in (2.8).⁷

For fixed interaction $V(l)$, the scaling properties of the weak-fluctuation regime hold for $d_1 > d > d_2$, where d_2 is determined from

$$|V_A(l)| \sim V_{\text{FL}}(l) \sim 1/l^{\tau(d)} \quad \text{as } l \rightarrow \infty \quad (3.46)$$

with $\tau(d)$ defined by (3.38). Thus, for the power-law interactions (2.4) and (2.5), d_2 follows from $r = \tau(d_2)$ which leads to

$$d_2 = (3r + 2)/(r + 2). \quad (3.47)$$

If $V_A(l)$ decays faster than any power as in (2.3), one has

$$d_2 = d_1 = d_0 = 3. \quad (3.48)$$

In such a situation, one may have several scaling regimes for fixed $d = 3$. Indeed, various regimes have been found for the short-range potential (2.3) within the linear renormalization group.^{17,18,7,19}

If one defines the critical exponent ν_\parallel via

$$\xi_\parallel \sim (W - W_c)^{-\nu_\parallel} \quad (3.49)$$

with $W_c = 0$ in the WFL regime ($d_1 > d > d_2$), one finds

$$\nu_\parallel = \frac{2}{2+r} \frac{1}{d-d_2}, \quad (3.50)$$

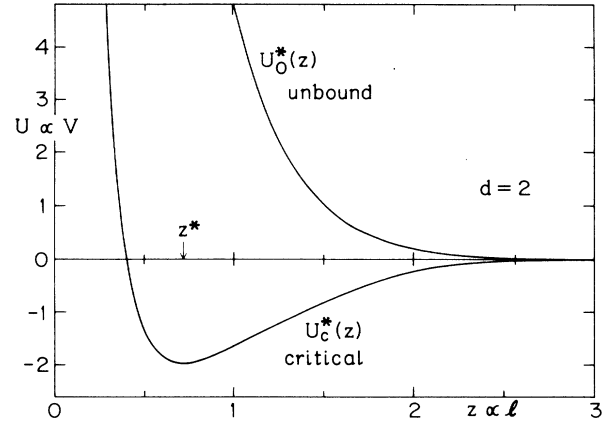


FIG. 4. The reduced fixed point potentials, $U_c^*(z)$, corresponding to the critical unbinding transition, and $U_0^*(z)$, describing the unbound, delocalized interface phase, for $d=2$ dimensions.

for unbinding in the long-range interface potential (2.4). Thus, $\nu_\parallel \rightarrow \infty$ as $d \rightarrow d_2 +$. One must then ask what happens for $d \leq d_2$, i.e., in the *strong-fluctuation* (SFL) regime in which

$$V_A(l)/V_{\text{FL}}(l) \sim V_A(l)l^\tau \rightarrow 0 \quad \text{for } l \rightarrow \infty. \quad (3.51)$$

The divergence of ν_\parallel as $d \rightarrow d_2 +$ at first seems to suggest that d_2 is the lower critical dimensionality and that there should be no transition for $d \leq d_2$. On the other hand, the minimization of $\Delta f \simeq V_R(l) + V_A(l) + V_{\text{FL}}(l)$ might still lead to a first-order transition if W in $V_A(l)$ is so large that Δf develops a second minimum at finite l which can compete with the minimum at $l = \infty$. Furthermore, exact calculations for $d=2$ show that, indeed, an unbinding transition remains present when $d \leq d_2$ but it is actually continuous rather than first-order!^{29,30} Apart from the marginal case $d=3$ with short-range interactions, there are no results for the SFL regime when $d \neq 2$ since all the perturbative techniques employed in the WFL regime fail for the SFL regime. In the remainder of the paper, we show, within a nonperturbative renormalization-group (RG) scheme that, for fixed dimensionality $d < d_0 = 3$, the critical points for all $V(l)$ satisfying (3.51) map onto the *same* nontrivial fixed-point potential, $V_c^*(l)$. Hence, the whole SFL regime is characterized by *universal* critical behavior. On the other hand, all potentials $V(l)$ satisfying (3.51) which lead to complete interfacial separation are mapped by the RG onto a *second* nontrivial fixed point, $V_0^*(l)$; this potential is purely repulsive, i.e., $V_0^*(l) > 0$ for all l , while the critical potential $V_c^*(l)$ has an attractive tail for large l ; see Fig. 4.

IV. RENORMALIZATION-GROUP APPROACH

A. Rescaling

A renormalization-group method involves a scale transformation of the spatial coordinates and of the fluctuating field. For the unbinding transitions studied here, the ap-

appropriate scale transformations are particularly simple as shown in this subsection.

At the transition point $W = W_c \geq 0$, the interface is no longer affected by the interaction with the wall, and as explained—see (3.6)—the difference correlation function behaves as

$$\Delta C(x) \approx (k_B T / \bar{\Sigma}) \Psi_0 |x|^{3-d}, \quad (4.1)$$

for $x \gg 1/\Lambda$ and $d < d_0 = 3$. Since one has

$$b^{2\xi} \Delta C(x/b) \approx \Delta C(x), \quad (4.2)$$

with $\xi = (3-d)/2$ by (3.13), the fluctuations are *invariant*, for length scales large compared to $1/\Lambda$, *under the scale transformation*

$$\mathbf{x} \rightarrow \mathbf{x}' = \mathbf{x}/b, \quad (4.3)$$

$$l \rightarrow l' = l/b^\xi. \quad (4.4)$$

This implies that the fluctuating field l does not have an anomalous dimension and, thus, that the critical point decay exponent is given simply by

$$\eta = 0. \quad (4.5)$$

In other words, there is *no* “wave-function renormalization”^{6,3,8} apart from the rescaling (4.4). Alternatively, one may consider the effective Hamiltonian (3.1) which is also invariant under the scale transformation (4.3) and (4.4) provided one does *not* rescale the interfacial stiffness $\bar{\Sigma}$. Indeed, the long-wavelength limit of $\bar{\Sigma}$ is *finite* for the systems considered here as discussed in Sec. II A. This is in contrast to a normal bulk critical point where the corresponding coefficient of the gradient term varies as ξ_η^η .

The scale invariance (4.2) holds at the transition point $W = W_c > 0$. It should also apply when W exceeds W_c but remains sufficiently close so that ξ_\parallel is large compared to $1/\Lambda$. Thus, the correlations should be scale invariant on the intermediate length scales given by $1/\Lambda \ll x \ll \xi_\parallel$. This expectation is fully confirmed by exact calculations for $d=2$.³ Thus, the scale transformation of *any* renormalization-group method when applied to continuous unbinding transitions should be given by (4.3) and (4.4). In the next section, we will describe a renormalization-group approach which embodies this property.

B. Nonlinear recursion relations

In this subsection, we describe the nonlinear recursion relations which we will use in order to investigate the interfacial model defined in Sec. II. These recursion relations are an extension of Wilson’s approximate recursion relations.¹⁰ In its original form, this renormalization group has been applied to various bulk critical phenomena. In this context, its major drawback is the fact that it *necessarily* leads to the vanishing of the critical exponent η . However, for the unbinding transitions studied here one has, indeed, $\eta=0$ as argued in the previous subsection. Therefore, these recursion relations are expected to be more reliable for the interfacial phase transitions considered here than for standard bulk critical phenomena.

One step of the RG consists of the following procedure.

First, the fluctuating interface coordinate l is divided into a short-wavelength and a long-wavelength part:

$$l(\mathbf{x}) = l^<(\mathbf{x}) + l^>(\mathbf{x}) \quad (4.6)$$

where $l^<$ and $l^>$ contain all Fourier components of l with wave numbers $|p| < \Lambda/b$ and $\Lambda/b < |p| < \Lambda$, respectively. Here, Λ is the high-momentum cutoff implicitly contained in the Hamiltonian (2.1), and $b > 1$ is the usual arbitrary spatial rescaling factor. The short-wavelength part $l^>(\mathbf{x})$ is now expanded in a complete set of suitably chosen eigenfunctions, $E_n(\mathbf{x})$, which are taken to be localized both in real space and in momentum space.¹⁰ In real space, these eigenfunctions are assumed to be localized within a cubic cell with volume Ω given by¹⁰

$$\begin{aligned} 1/\Omega(b) &\equiv \int_{\Lambda/b}^{\Lambda} d^{d-1}p / (2\pi)^{d-1} \\ &= 2(1-b^{1-d})\Lambda^{d-1} / (4\pi)^{(d-1)/2} (d-1) \Gamma\left[\frac{d-1}{2}\right] \\ &= \begin{cases} (1-b^{-2})\Lambda^2 / 4\pi & \text{for } d=3 \\ (1-b^{-1})\Lambda / \pi & \text{for } d=2. \end{cases} \end{aligned} \quad (4.7)$$

In momentum space, on the other hand, they are supposed localized within the momentum shell $\Lambda/b < |p| < \Lambda$.³¹

Now, the trace over the short-wavelength fluctuations, $l^>(\mathbf{x})$, is performed in an approximate way. The various approximations involved have been described previously in the literature in some detail,^{10,32} so we will not repeat them here. The partial trace over $l^>(\mathbf{x})$ leads to a new Hamiltonian with momentum cutoff Λ/b . In order to bring this cutoff back to its original value Λ , the coordinate \mathbf{x} is rescaled according to $\mathbf{x} \rightarrow \mathbf{x}' = \mathbf{x}/b$. At the same time, the fluctuations are also rescaled by putting

$$l(\mathbf{x}') \equiv l^<(\mathbf{x} = b\mathbf{x}') / b^\xi \quad (4.8)$$

with $\xi = \frac{1}{2}(3-d)$ as in (3.13). Note that this is just the scale transformation (4.3) and (4.4) which, as mentioned, must apply at an unbinding fixed point even in an exact RG method. As a consequence, the gradient term in (2.1) remains unchanged and the RG acts only in the function space of nongradient interactions as represented by the potential $V(l)$.

In order to write the recursion relation for the potential in the most transparent way, we recall (4.7) and introduce the scale

$$\bar{v}(b) \equiv k_B T / \Omega(b), \quad (4.9)$$

for the free-energy density, and the length scale, $\bar{a}(b)$, defined by

$$\begin{aligned} \bar{a}^2(b) &= \frac{k_B T}{\bar{\Sigma}} \int_{\Lambda/b}^{\Lambda} d^{d-1}p / (2\pi)^{d-1} p^2 \\ &= \frac{k_B T}{\bar{\Sigma}} \frac{2\pi^{(d-1)/2} \Lambda^{d-3} (b^{3-d} - 1)}{(2\pi)^{d-1} \Gamma(\frac{1}{2}(d-1)) (3-d)} \\ &= \begin{cases} (k_B T / \bar{\Sigma})(b-1) / \pi \Lambda & \text{for } d=2 \\ (k_B T / 2\pi \bar{\Sigma}) \ln b & \text{for } d=3. \end{cases} \end{aligned} \quad (4.10)$$

Comparison with (3.16) and (3.2) shows that the length scale \bar{a} can be viewed as the interfacial roughness arising from short-wavelength fluctuations. Then, the initial potential $V^{(0)}(l) \equiv V(l)$ is renormalized according to

$$V^{(1)}(l) = \mathcal{R}[V^{(0)}(l)] \quad (4.11)$$

with

$$\mathcal{R}[V(l)] \equiv -\bar{v}b^{d-1} \ln \left[\int_{-\infty}^{\infty} \frac{dl'}{\sqrt{2\pi\bar{a}}} \times \exp\left[-\frac{1}{2}(l'/\bar{a})^2 - G(l, l')\right] \right], \quad (4.12)$$

where the potential enters through

$$G(l', l) \equiv [V(b^{\xi}l - l') + V(b^{\xi}l + l')]/2\bar{v} \quad (4.13)$$

in which $\xi = \frac{1}{2}(3-d)$ as before.

Compared to Wilson's original method,¹⁰ the new features of our RG are: (a) the normalization of the integral in (4.12), which has been set to preserve the form of $V(l)$ for large l as required for interface problems; (b) the specific definition of the length scale $\bar{a}(b)$ which was originally treated as arbitrary;¹⁰ it transpires that the choice (4.10) ensures that our RG is *exact* to linear order in V for all b and d ; see Sec. IV C below; (c) the trivial "wavefunction renormalization" as given by (4.8) and embodied in (4.13) is to be regarded as exact in the present context, as discussed in Sec. III A above.

In the infinitesimal rescaling limit $b = e^{\delta t}$ ($\delta t \rightarrow 0$) the recursion relation (4.11) leads to a relatively simple flow equation. If one takes the b dependence of the scale factors $\bar{v}(b)$ and $\bar{a}(b)$ into account, one finds from a straightforward calculation that this nonlinear flow equation is

$$\frac{dV}{dt} = (d-1)V + \zeta l \frac{\partial V}{\partial l} + \frac{1}{2}B \ln \left[1 + \frac{A^2}{B} \frac{\partial^2 V}{\partial l^2} \right], \quad (4.14)$$

with the b -independent length parameter

$$A \equiv \left[\frac{\bar{a}^2(3-d)}{b^{3-d-1}} \right]^{1/2} = \left[\frac{k_B T}{\bar{\Sigma}} \frac{2\pi^{(d-1)/2} \Lambda^{d-3}}{(2\pi)^{d-1} \Gamma(\frac{1}{2}(d-1))} \right]^{1/2} \quad (4.15)$$

and energy scale

$$B \equiv \frac{\bar{v}(d-1)}{1-b^{1-d}} = \frac{2\Lambda^{d-1}k_B T}{(4\pi)^{(d-1)/2} \Gamma(\frac{1}{2}(d-1))}. \quad (4.16)$$

For bulk critical phenomena, an approximate RG flow equation equivalent to (4.14) has been recently derived and examined independently by Hasenfratz and Hasenfratz.³³

C. Linearized recursion relations

In this subsection, we show that the recursion relation (4.11) is *exact* to first order in the potential as a consequence of the choice (4.10) for $\bar{a}(b)$. The linearized recursion relation which follows from (4.11)–(4.13) is

$$V_{\text{lin}}^{(N+1)}(l) = b^{d-1} \int_{-\infty}^{\infty} \frac{dl'}{\sqrt{2\pi\bar{a}}} e^{-l'^2/2a^2} V^{(N)}(b^{\xi}l - l'). \quad (4.17)$$

Note that the factor $\bar{v}(b)$, which depends on the volume Ω of the cells in real space, has dropped out here. Now, if $V^{(N)}(l)$ has a Taylor expansion in l , one can rewrite this linearized recursion relation as

$$\begin{aligned} V_{\text{lin}}^{(N+1)}(l) &= b^{d-1} \int_{-\infty}^{\infty} \frac{dl'}{\sqrt{2\pi\bar{a}}} \\ &\quad \times \exp\left[-\frac{1}{2}(l'/\bar{a})^2 - l' \frac{d}{dz}\right] V^{(N)}(z) \\ &= b^{d-1} \exp\left[\frac{1}{2}\bar{a}^2 \frac{d^2}{dz^2}\right] V^{(N)}(z), \end{aligned} \quad (4.18)$$

where we have put

$$z \equiv b^{\xi}l. \quad (4.19)$$

On the other hand, one may obtain the exact linear RG by an explicit integration over the short-wavelength fluctuations.⁷ In order to do this, let us first rewrite the reduced interface Hamiltonian as

$$\mathcal{H}\{l\} = \mathcal{H}_0\{l\} + \mathcal{H}_1\{l\}, \quad (4.20)$$

with terms

$$\mathcal{H}_0\{l\} = \int d^{d-1}x \frac{1}{2} \bar{\Sigma} (\nabla l)^2 / k_B T, \quad (4.21)$$

$$\mathcal{H}_1\{l\} = \int d^{d-1}x V^{(N)}(l) / k_B T. \quad (4.22)$$

Now, we divide $l(\mathbf{x})$ into a short-wavelength and a long-wavelength part as in (4.6). Since $l^>$ and $l^<$ have, by definition, no common Fourier component, one has

$$\mathcal{H}_0\{l^< + l^>\} = \mathcal{H}_0\{l^<\} + \mathcal{H}_0\{l^>\}. \quad (4.23)$$

The intermediate, unrescaled, renormalized Hamiltonian is defined as usual via the partial trace:

$$\exp[-\mathcal{H}'\{l^<\}] \equiv N_0^{-1} \int \mathcal{D}l^> \exp[-\mathcal{H}\{l^< + l^>\}] \quad (4.24)$$

with normalization

$$N_0 = \int \mathcal{D}l^> \exp[-\mathcal{H}_0\{l^>\}]. \quad (4.25)$$

On using (4.23), this leads to

$$\exp[-\mathcal{H}'\{l^<\}] = \exp[-\mathcal{H}_0\{l^<\}] \left[1 - N_0^{-1} \int \mathcal{D}l^> e^{-\mathcal{H}_0\{l^>\}} \mathcal{H}_1\{l^< + l^>\} + \mathcal{O}(\mathcal{H}_1^2) \right]. \quad (4.26)$$

Assuming again that $V^{(N)}(l)$ has a Taylor expansion the integration over $l^>$ can now be performed explicitly to give

$$N_0^{-1} \int \mathcal{D}l^> e^{-\mathcal{H}_0[l^>]} V^{(N)}(l^< + l^>) \\ = \exp \left[\frac{1}{2} \bar{a}^2 \frac{d^2}{dl^2} \right] V^{(N)}(l^<), \quad (4.27)$$

with $\bar{a}^2(b)$ as given by (4.10). Therefore, up to first order in the interaction potential V (or \mathcal{H}_1), (4.26) leads to

$$\mathcal{H}'\{l^<\} = \mathcal{H}_0\{l^<\} + \int d^{d-1}x \exp \left[\frac{1}{2} \bar{a}^2 \frac{d^2}{dl^2} \right] V^{(N)}(l^<). \quad (4.28)$$

Finally, one must rescale \mathbf{x} and l as before, via $\mathbf{x} \rightarrow \mathbf{x}' \equiv \mathbf{x}/b$ and $l(\mathbf{x}') \equiv l^<(\mathbf{x} = b\mathbf{x}')/b^\xi$; see (4.3) and (4.4). As a result, (4.28) reduces to the expression (4.18) for the renormalized potential $V_{\text{lin}}^{(N+1)}(l)$ computed to linear order from (4.11)–(4.13).

Thus, to first order in the interaction potential V , the recursion relation (4.11) reduces to (4.18) which is exact for *arbitrary* rescaling factor $b > 1$. It follows that our linearized RG has the appropriate semigroup property as can be checked easily by use of (4.18) and the identity

$$\bar{a}^2(b_1)b_2^{3-d} + \bar{a}^2(b_2) = \bar{a}^2(b_1b_2), \quad (4.29)$$

which follows from (4.10). For infinitesimal rescaling factor $b = e^{\delta t}$ ($\delta t \rightarrow 0$), the linear recursion relation (4.18) leads to the flow equation

$$\frac{dV}{dt} = (d-1)V(l) + \xi l \frac{dV}{dl} + \frac{1}{2} A^2 \frac{d^2}{dl^2} V(l), \quad (4.30)$$

where A^2 is given in (4.15). This equation was the basis of the study by Fisher and Huse⁷ who denoted $\frac{1}{2}A^2$ by $1/\bar{\sigma} \equiv \omega \xi_\infty^2$, where ξ_∞ is the bulk correlation length.

D. Dimensionless variables

In the balance of this paper, we study the discrete nonlinear recursion relations with fixed $b > 1$, usually taking $b=2$. It is then convenient to absorb the scale factors $\bar{a}(b)$ and $\bar{v}(b)$ in (4.10) and (4.9) into the potential. Thus, let us define the rescaled quantities

$$z \equiv l/\sqrt{2}\bar{a}(b), \quad U^{(N)}(z) \equiv V^{(N)}[\sqrt{2}\bar{a}(b)z]/\bar{v}(b). \quad (4.31)$$

Both U and z are dimensionless; however, since both \bar{a} and \bar{v} depend on b , the rescaling also depends on b .

The full nonlinear recursion function (4.12) now becomes

$$U^{(N)}(z) = \bar{\mathcal{R}}[U^{(N-1)}(z)] \\ \equiv -b^{d-1} \ln \left[(2/\sqrt{\pi}) \int_0^\infty dy e^{-y^2 - K(y,z)} \right], \quad (4.32)$$

with kernel

$$K(y,z) \equiv \frac{1}{2} U^{(N-1)}(b^\xi z - y) + \frac{1}{2} U^{(N-1)}(b^\xi z + y), \quad (4.33)$$

where $\xi = \frac{1}{2}(3-d)$, as before, and the symmetry $K(-y,z) = K(y,z)$ has been used in order to restrict the integration in (4.32) to $y > 0$. The *linearized* recursion relation which follows from this is given by

$$U_{\text{lin}}^{(N)}(z) = b^{d-1} \int_{-\infty}^\infty \frac{dy}{\sqrt{\pi}} e^{-y^2} U^{(N-1)}(b^\xi z - y). \quad (4.34)$$

The same recursion relation follows directly from (4.18) via the scale transformation (4.31). One should note, however, that the full semigroup property (i.e., for arbitrary b) is *not* possessed by (4.34) because of the implicit dependence of z on b .

E. Hard wall potentials

It has been emphasized in Sec. II B that negative values of l are unphysical and that one should ideally study a hard wall, i.e., $V^{(0)}(l) = \infty$ for $l < 0$ which, via (4.31) implies $U^{(0)}(z) = \infty$ for $z < 0$. Such a wall cannot be handled by the linearized recursion relation since (4.34) would lead to $U_{\text{lin}}^{(1)}(z) = \infty$ for *all* z if $U^{(0)}(z) = \infty$ for $z < 0$. On the other hand, a hard wall is easily handled by the nonlinear recursion relation. Indeed, it is not difficult to see from (4.32) that the hard wall remains fixed at $z=0$ under subsequent iterations of this nonlinear recursion relation, i.e., one has

$$U^{(N)}(z) = \infty, \quad \text{for } z < 0, \quad (4.35)$$

for all N if the relation holds for $N=0$. For $z > 0$, on the other hand, (4.35) and (4.32) yield

$$U^{(N)}(z) = -b^{d-1} \ln \left[\frac{2}{\sqrt{\pi}} \int_0^{b^\xi z} dy e^{-y^2 - K(y,z)} \right] \quad (4.36)$$

with $K(y,z)$ still given by (4.33). Thus, compared to (4.32), the only effect of the hard wall is to introduce the upper limit $b^\xi z$ on the y integration.

V. SOME BOUNDS FOR THE NONLINEAR RECURSION RELATION

In this section, we establish some general properties of the nonlinear recursion relations (4.32) and (4.36). Consider, first, two initial potentials, $U^{(0)}$ and $P^{(0)}$, satisfying

$$\Delta(z) \equiv U^{(0)}(z) - P^{(0)}(z) \leq 0 \quad (\text{all } z). \quad (5.1)$$

We may now define the ‘‘partition function’’

$$Q_\alpha(l) \equiv \frac{2}{\sqrt{\pi}} \int_0^{b^\xi z} dy e^{-y^2 - K(y,z) - \alpha \bar{K}(y,z)}, \quad (5.2)$$

with $K(y,z)$ as in (4.33) but with $U^{(N)}$ replaced by $P^{(0)}$ and

$$\bar{K}(y,z) \equiv \frac{1}{2} \Delta(b^\xi z - y) + \frac{1}{2} \Delta(b^\xi z + y) \leq 0. \quad (5.3)$$

The corresponding free energy is

$$F_\alpha(z) \equiv -b^{d-1} \ln[Q_\alpha(z)]. \quad (5.4)$$

Comparison with the recursion relation (4.36) shows that one has

$$F_0 = P^{(1)} \quad \text{and} \quad F_1 = U^{(1)}. \quad (5.5)$$

Furthermore, it follows from Schwarz's inequality that F_α is *convex upwards* as a function of α ,³⁴ which implies

$$F_1 \leq F_0 + (\partial F / \partial \alpha)_0. \quad (5.6)$$

However, the relations (5.2)–(5.4) yield

$$(\partial F / \partial \alpha)_0 \leq 0. \quad (5.7)$$

Combining this with (5.5) then gives the inequality $U^{(1)}(z) \leq P^{(1)}(z)$ (all z) so that the nonlinear recursion relation *preserves* the original inequality $U \leq P$. Finally, iterating N times gives

$$U^{(N)}(z) \leq P^{(N)}(z), \quad (5.8)$$

which is valid for all $N > N_0$ if it holds for $N = N_0$.

A. Upper bound

Let us define the further partition function

$$\bar{Q}_\beta(z) \equiv \frac{2}{\sqrt{\pi}} \int_0^{b^{\xi}z} dy e^{-y^2 - \beta K(y,z)} \quad (5.9)$$

and the corresponding free energy \bar{F}_β as in (5.4). Evidently, we have

$$\bar{F}_1(z) = U^{(1)}(z), \quad (5.10)$$

where $U^{(1)}(z)$ is the result of applying the recursion relation (4.36) once. For $\beta=0$, on the other hand, one obtains

$$\bar{F}_0(z)/b^{d-1} = S(b^{\xi}z) \equiv -\ln \left[\frac{2}{\sqrt{\pi}} \int_0^{b^{\xi}z} dy e^{-y^2} \right]. \quad (5.11)$$

It follows again from Schwarz's inequality that \bar{F}_β is *convex upwards* as a function of β so that

$$\bar{F}_1 \leq \bar{F}_0 + (\partial \bar{F} / \partial \beta)_0. \quad (5.12)$$

Thence (5.10) and (5.11) yield the bound

$$U^{(1)}(z) \leq b^{d-1} S(b^{\xi}z) + b^{d-1} \exp[S(b^{\xi}z)] \int_{-b^{\xi}z}^{b^{\xi}z} \frac{dy}{\sqrt{\pi}} e^{-y^2} U^{(0)}(b^{\xi}z - y). \quad (5.13)$$

In the *absence* of a hard wall, one must extend the integration range to $(-\infty, \infty)$ and replace $S(b^{\xi}z)$ by $S(\infty)=0$. This leads to

$$U^{(1)}(z) \leq U_{\text{lin}}^{(1)}(z), \quad (5.14)$$

where the right-hand side represents the result of using the linearized recursion (4.34). In terms of the original interaction potential $V(l)$, this becomes

$$V^{(1)}(l) \leq V_{\text{lin}}^{(1)}(l), \quad (5.15)$$

with V_{lin} determined by (4.18). As mentioned, the linear recursion relation for V has the semigroup property. Therefore, N applications of this bound lead to

$$V^{(N)}(l) \leq b^{N(d-1)} \int_{-\infty}^{\infty} \frac{dl'}{\sqrt{2\pi \bar{a}_N}} \exp[-\frac{1}{2}(l'/\bar{a}_N)^2] \times V^{(0)}(b^{N\xi}l - l'), \quad (5.16)$$

where \bar{a}_N is related to \bar{a} in (4.10) by

$$\bar{a}_N^2(b) \equiv \bar{a}^2(b)(b^{N(3-d)} - 1)/(b^{3-d} - 1). \quad (5.17)$$

B. Lower bound

A lower bound for $U^{(1)}(z)$ can be obtained from a lower bound for the kernel $K(y,z)$. Thus, if one has

$$K(y,z) \geq B(y,z), \quad (5.18)$$

one may conclude from (4.32) in the presence of a hard wall,

$$U^{(1)}(z) \geq -b^{d-1} \left[\frac{2}{\sqrt{\pi}} \int_0^{b^{\xi}z} dy e^{-y^2 - B(y,z)} \right], \quad (5.19)$$

Furthermore, if $U^{(0)}(z)$ is *convex downwards* as a function of z , one has from (4.33), by definition,

$$K(y,z) \equiv \frac{1}{2} U^{(0)}(b^{\xi}z - y) + \frac{1}{2} U^{(0)}(b^{\xi}z + y) \geq U^{(0)}(b^{\xi}z) \equiv K(0,z). \quad (5.20)$$

Then, (5.19) leads to

$$U^{(1)}(z) \geq b^{d-1} U^{(0)}(b^{\xi}z) + b^{d-1} S(b^{\xi}z), \quad (5.21)$$

where $S(x)$ is defined by (5.11). In the *absence* of a hard wall, this simplifies further: the last term may be dropped because $S(\infty)=0$.

Not all the interface potentials of interest to us are *convex downwards* for all values of z . Nevertheless we may obtain bounds valid near a hard wall even for potentials which have an attractive well and vanish for large z . Thus, suppose $(\partial^2 U / \partial z^2) \geq 0$ for $0 \leq z \leq z_0$. The inequality (5.20) is then valid for $b^{\xi}z + y \leq z_0$; furthermore, for a hard wall we have $y \leq b^{\xi}z$. Thus (5.20) and thence (5.21) remain valid for $0 \leq z \leq z_0/2b^{\xi}$.

We learn from these bounds that the nonlinearities of the full recursion relation are relatively weak. For example, for interface potentials $V^{(0)}$ which are *convex downwards* and have no hard wall, a combination of (5.15) and (5.21) implies

$$b^{d-1} V^{(0)}(b^{\xi}l) \leq V^{(1)}(l) \leq V_{\text{lin}}^{(1)}(l). \quad (5.22)$$

Furthermore, for potentials without a hard wall as studied in Refs. 17 and 7, the upper bounds (5.15) and (5.16) have a direct consequence for the phase diagram of the unbinding transition. As explained in the next section, the bound or localized phase of the interface corresponds to a RG flow in which the potential well becomes deeper and deeper. Therefore, these upper bounds imply that the full recursion relation predicts a localized state of the interface

whenever the linearized recursion relation leads to the same conclusion. Finally, the bounds described in this section provide useful checks on the accuracy of numerical iterations of the full recursion relation.

VI. STRONG FLUCTUATION REGIME: NUMERICAL STUDY

In this section, we will describe a numerical study based on the nonlinear recursion relation (4.32) for initial potentials $U^{(0)}(z) = V^{(0)}(\sqrt{2}az)/\bar{v}$ which satisfy (3.51) and, thus, belong to the SFL regime. This reveals the existence of *two* nontrivial fixed points for $d < 3$, as illustrated in Fig. 4. These fixed points describe the critical manifold and the completely delocalized phase, respectively.

A. Numerical determination of fixed points

A fixed point, $U^*(z)$, of the recursion relation (4.32) satisfies

$$U^*(z) = \bar{\mathcal{R}}[U^*(z)]. \quad (6.1)$$

However, it is important to realize that this relation reflects the choice of origin for z . It follows from (4.32) that a translation, $z \rightarrow z - \Delta z$, leads to

$$\bar{\mathcal{R}}[U^*(z - \Delta z)] = U^*(z - \Delta z / b^\xi). \quad (6.2)$$

To first order in Δz , this yields

$$\bar{\mathcal{R}} \left[U^*(z) - \Delta z \frac{\partial U^*}{\partial z} \right] = U^*(z) - b^{-\xi} \Delta z \frac{\partial U^*}{\partial z}, \quad (6.3)$$

which implies the presence of a RG eigenperturbation with scaling index

$$\lambda_2 = -\xi = -\frac{1}{2}(3-d). \quad (6.4)$$

For $d < 3$ and $d = 3$, one has $\lambda_2 < 0$ and $\lambda_2 = 0$ and so this perturbation is *irrelevant* and *marginal*, respectively.

It is found numerically that λ_2 is the leading negative scaling index for all $d < 3$ provided the initial potential $U^{(0)}(z)$ decays to zero for large z faster than any power law. In this case, the vicinity of a fixed point can be conveniently found numerically by using the observation that the RG acts like a simple translation, as in (6.2). In this way, two fixed-point potentials, $U_0^*(z)$ and $U_c^*(z)$, have been determined for various dimensionalities in the range $2 \leq d < 3$. Some of the results are shown in Fig. 4 and Fig. 6, below.

The fixed point $U_0^*(z)$ for the delocalized phase is easy to find numerically since it is completely stable within the space of potentials which belong to the SFL regime as specified by (3.51). Thus, within this space, the fixed point U_0^* has a domain of attraction of codimension zero: one may thus start with any purely repulsive potential or with any potential which has a sufficiently small minimum and under iteration the potential $U_0^*(z)$ will be approached. Once one gets sufficiently close, the RG no longer affects the *shape* of the potential but merely shifts it according to (6.2), so that

$$U^{(N+1)}(z) = \bar{\mathcal{R}}[U^{(N)}(z)] \simeq U^{(N)}(z - \Delta_1). \quad (6.5)$$

It then follows from (6.2) that further iterations of the recursion relation lead to

$$U^{(N+J)}(z) = \bar{\mathcal{R}}^J[U^{(N)}(z)] \simeq U^{(N)}(z - \Delta_J) \quad (6.6)$$

with

$$\Delta_J \equiv \sum_{j=1}^J \Delta_1 / b^{(j-1)\xi}. \quad (6.7)$$

Since the shape remains (essentially) unchanged one may say that one has attained a “drifting” fixed point. However, for $d < 3$, the successive shifts decay as $b^{-\xi}$ and one will eventually attain a true or “stationary” fixed point. Once the drifting fixed-point regime is attained the stationary fixed point may be well estimated by

$$U_0^*(z) \simeq U^{(N)}(z - \Delta_\infty) \quad (6.8)$$

with

$$\Delta_\infty = \frac{b^\xi}{b^\xi - 1} \Delta_1. \quad (6.9)$$

Thus, in practice, one may stop iterating the RG once (6.6) is well satisfied and then use (6.8) and (6.9) to determine the fixed point. Note, however, that Δ_∞ diverges when $d \rightarrow 3$ — since $\xi = \frac{1}{2}(3-d)$. This reflects the fact that the translation becomes a marginal perturbation when $d = 3$.

The second fixed point, $U_c^*(z)$, is more difficult to determine numerically since its domain of attraction has codimension one, i.e., there is *one relevant perturbation* within the SFL regime specified by (3.51). Consequently, in order to find $U_c^*(z)$ one must systematically vary one parameter, say p , of the initial potential $U^{(0)}(z)$ until this potential comes close to the attractive manifold of U_c^* , which represents the critical-unbinding transition surface. Then, as a function of p , the iterated potentials $U^{(N)}$ for large N are observed to exhibit three types of behavior: (i) for a critical value $p = p_c$, the potential $U^{(N)}$ is eventually mapped onto the fixed point U_c^* . In numerical calculations, this behavior can be maintained only for a limited number of iterations owing to the effects of numerical roundoff; (ii) for $p > p_c$, say, the minimum of $U^{(N)}$ becomes deeper and deeper: this behavior describes, as in bulk critical phenomena,^{10,32} an “ordered” or bound phase in which the interfacial separation remains finite; (iii) for $p < p_c$, on the other hand, the attractive part of $U^{(N)}$ decays to zero, and $U^{(N)}$ is eventually mapped onto the repulsive fixed point U_0^* which describes the completely unbound phase.

We have implemented this procedure in a detailed study of the RG trajectories for initial potentials of the form

$$U^{(0)}(z) = \begin{cases} -we^{-sz} + e^{-2sz} & \text{for } z > 0, \\ \infty & \text{for } z < 0, \end{cases} \quad (6.10)$$

which are a special case of (2.3) when rescaled according to (4.31). In this case, one may vary either the parameter w or s . This leads to a separatrix *alias* a critical locus, $w = w_c(s)$, which divides the (s, w) plane into two parts as shown in Fig. 5 for various values of the dimensionality d .

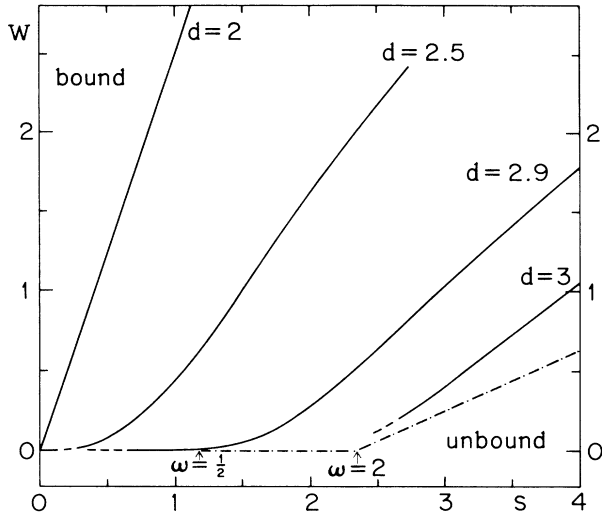


FIG. 5. Critical loci in the (w, s) plane for the potential $U^{(0)}(z)$ given by (6.10) for various dimensionalities, d , calculated numerically from the approximate functional renormalization group with $b=2$. The dotted-dashed lines indicate the critical loci expected for $d=3$ on the basis of the linearized functional renormalization group as studied by Huse and Fisher (Ref. 7); the values of s marked by $\omega = \frac{1}{2}$ and $\omega = 2$ indicate the distinct critical regimes emerging in that analysis (see also Refs. 17 and 18).

For comparison, Fig. 5 also contains the phase boundary obtained from the linear RG in $d=3$ when applied to initial potentials as in (6.10) but with a “finite wall” that is $U^{(0)}(z)=c$ for $z < 0$.⁷ The slope of this boundary depends on c : for larger values of c , it intersects the phase boundary obtained from the full, nonlinear RG and becomes parallel to the w axis when $c \rightarrow \infty$.

For $w > w_c(s)$ the interfaces are bound and the potential minimum of $U^{(N)}$ increases for large N . For $w < w_c(s)$, the interfaces are unbound or delocalized and the initial potential is eventually mapped onto the fixed point $U_0^*(z)$. Finally, for $w \simeq w_c(s)$, the potentials $U^{(N)}(z)$ for intermediate N remain close to the fixed point U_c^* which may thus be estimated with reasonable precision.

The two stationary fixed points for $d=2$ and $d=2.8$ as determined numerically for rescaling factor $b=2$ are displayed in Figs. 4 and 6. The behavior for general $d < 3$ is similar. The decay to zero at large values of z is always observed to be faster than exponential. Indeed, one can show that in the infinitesimal rescaling limit $b = e^{\delta t}$ ($\delta t \rightarrow 0$), the fixed-point potentials have a Gaussian tail. This follows from the differential recursions relation (4.14) which leads to

$$(d-1)V^* + \zeta l \frac{\partial V^*}{\partial l} + \frac{1}{2} B \ln \left[1 + \frac{A^2}{B} \frac{\partial^2 V^*}{\partial l^2} \right] = 0 \quad (6.11)$$

for a (stationary) fixed point V^* . For large l , $V^*(l)$ is small and the linear equation

$$(d-1)V^* + \zeta l \frac{\partial V^*}{\partial l} + \frac{1}{2} A^2 \frac{\partial^2 V^*}{\partial l^2} = 0 \quad (6.12)$$

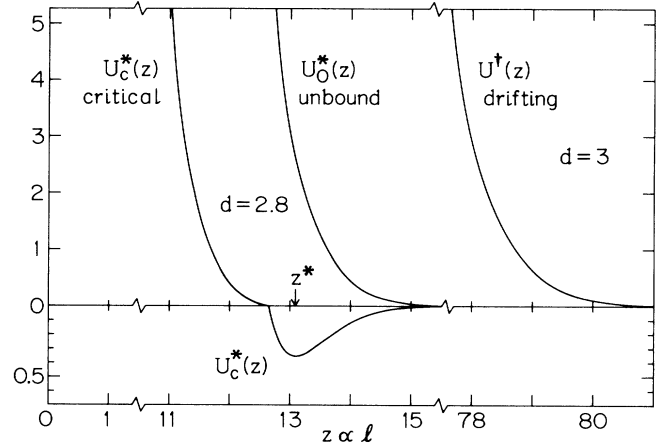


FIG. 6. Reduced fixed-point potentials, $U_c^*(z)$ and $U_0^*(z)$, in dimensionality $d=2.8$ (compare with Fig. 4) and the “drifting fixed-point” potential, $U^\dagger(z)$, remaining in $d=3$, which is wholly positive. Note the breaks in the z axis; the location of the drifting fixed-point potential has no special significance.

must describe the decay. A balance of the first and the second term leads to $V^*(l) \sim l^{-\tau}$ with $\tau = 2(d-1)/(d-3)$ [see (3.38)]. This behavior of V^* is, however, not possible within the SFL regime as specified by (3.51). A balance of the first and the third term does not lead to a function V^* which decays to zero for large l . Finally, if the last two terms in (6.12) are balanced, one obtains the Gaussian decay

$$\frac{\partial V^*(l)}{\partial l} \sim \exp(-\zeta l^2/A^2) \text{ as } l \rightarrow \infty, \quad (6.13)$$

with A^2 given in (4.15). This must represent the asymptotic behavior of both fixed points $V_0^*(l)$ and $V_c^*(l)$ for $d < 3$. Likewise, via (4.31) and (4.15), both $U_0^*(z)$ and $U_c^*(z)$ should decay as

$$\exp[-2\zeta(\bar{a}z/A)^2] = \exp[-(b^{3-d}-1)z^2]$$

for $d < 3$ when $b \rightarrow 1$.

B. Fixed-point potentials in the vicinity of $d=3$

For $d=3$ and $\zeta=0$, the relation (6.2) becomes

$$\bar{\mathcal{R}}[U^*(z - \Delta z)] = U^*(z - \Delta z), \quad (6.14)$$

valid for any value of Δz . Therefore, the existence of one true or stationary fixed point would imply a whole line of such fixed points. However, this scenario is *not* realized in actuality as can be shown with the aid of the differential recursion relation (4.14). For $\zeta=0$, this simplifies to

$$\frac{\partial V}{\partial t} = (d-1)V + \frac{1}{2} B \ln \left[1 + \frac{A^2}{B} \frac{\partial^2 V}{\partial l^2} \right] \quad (6.15)$$

with A and B given by (4.15) and (4.16). Now, a (stationary) fixed point entails $\partial V/\partial t = 0$ which leads to

$$\frac{\partial^2 V}{\partial l^2} = \frac{B}{A^2} \left[\exp \left[-\frac{2(d-1)}{B} V \right] - 1 \right] \equiv -\frac{\partial \Phi(V)}{\partial V}. \quad (6.16)$$

This equation can be viewed as the conservative motion of a classical particle with positional coordinate V moving with time l in a potential

$$\Phi(V) = \frac{B^2}{2(d-1)A^2} \exp \left[-\frac{2(d-1)}{B} V \right] + \frac{B}{A^2} V \quad (6.17)$$

which is convex downwards with a unique minimum at $V=0$. Now, the boundary condition for large “times” l is

$$V(l) \rightarrow 0 \text{ for } l \rightarrow \infty. \quad (6.18)$$

Therefore, the particle must eventually reach the minimum of $\Phi(V)$. However, this is impossible unless $V(l)=0$ for all l since (6.16) conserves the energy functional $E = \frac{1}{2}(\partial V/\partial l)^2 + \Phi(V)$ for all l . Thus, the only true fixed point in $d=3$ is the trivial fixed point $V^*(l)=0$ or $U^*(z)=0$. For $b>1$ the numerical studies confirm the identical conclusion; it can probably also be established analytically.

Even though no true nontrivial fixed points exist when $d=3$, numerical iterations reveal a line of *drifting fixed points*, $U^\dagger(z)$, which satisfy the defining relation

$$\overline{\mathcal{R}}[U^\dagger(z)] = U^\dagger(z - \Delta z^*), \quad (6.19)$$

with $\Delta z^* > 0$. For $b=2$, we find $\Delta z^* = 1.168$. As evident from Fig. 6, these drifting fixed points prove to be completely repulsive, i.e., $U^\dagger(z) \geq 0$.

It is clearly of interest from an analytic point of view to inquire how this behavior in $d=3$ connects to that found for $d < 3$. Specifically, as

$$\epsilon \equiv 3 - d \quad (6.20)$$

approaches zero from below, the fixed points $U_0^*(z)$ and $U_c^*(z)$ exhibit a special character which indicates that they *bifurcate from the line of drifting fixed points* in $d=3$. In the coordinate system in which the two fixed points U_0^* and U_c^* are stationary, their position, as measured, say, by the location of the minimum or some fixed, positive value of U , moves out towards infinite z as $\epsilon \rightarrow 0$. To study this quantitatively the location, z^* , of the minimum of $U_c^*(z)$ is listed in Table I for rescaling factor $b=2$ and

various values of d . One finds that

$$z^*(d) \approx Z_0/\epsilon \text{ as } \epsilon \rightarrow 0^-, \quad (6.21)$$

with $Z_0 \approx 3.34$ ($b=2$). [Note that (4.31) and (4.10) imply $l \approx z(k_B T \ln b / \sqrt{2\pi\tilde{\Sigma}})^{1/2}$ when $d \rightarrow 3$.] Similarly, it is convenient to define the abscissae z_k^0 and z_k^c via

$$U_0^*(z_k^0) = U_c^*(z_k^c) = k \geq 0.$$

Table I lists z_1^0 which is found to diverge like (6.21) with the *same* value of Z_0 ; indeed, the difference $z_1^0 - z^*$ appears to approach a fixed value close to 0.14 when $d \rightarrow 3$.

As the fixed point potentials $U_0^*(z)$ and $U_c^*(z)$ move outwards, the shape of their *repulsive* parts become increasingly close to the shape of the drifting fixed point $U^\dagger(z)$. This can be gauged qualitatively from Fig. 6 and can be evaluated quantitatively by noting the smooth evolution of the shape-sensitive differences

$$\Delta z_{k,k'}^0 = z_k^0 - z_{k'}^0 \quad \text{and} \quad \Delta z_{k,k'}^c = z_k^c - z_{k'}^c,$$

as $d \rightarrow 3$; see Table I and note that the values shown for $d=3$ correspond to $U^\dagger(z)$. On the other hand, although the minimum of U_c^* remains close to the steeply rising part of U_0^* —recall that $z_1^0 - z^* \approx 0.14$ as $d \rightarrow 3$ —the repulsive parts of U_c^* and U_0^* actually drift apart when $d \rightarrow 3$. This can be seen from the differences $\Delta z_k^* = z_k^0 - z_k^c$, listed in Table I, which appear to diverge roughly as $\Delta z_k^* \approx \Delta Z/\epsilon^{1/3}$ when $\epsilon \rightarrow 0$, with $\Delta Z \approx 1.5$ independent of k . [There may well be logarithmic factors present in the divergence of Δz_k^* see (6.22) and (6.33) below.]

While the repulsive part of $U_c^*(z)$ approaches the drifting fixed point $U^\dagger(z)$ the *attractive* part exhibits a scaling behavior. The depth $U_{c,\min}^* \equiv U_c^*(z^*)$ rapidly decreases as $\epsilon \rightarrow 0$; see Table I. The numerical values displayed in this table for rescaling factor $b=2$ are well fit by the expression⁹

$$U_{c,\min}^* \approx -A_c \epsilon^3 / [\ln(B_c/\epsilon) + C_c \epsilon]^{1/2} \quad (6.22)$$

with $A_c = \sqrt{51}$, $B_c = 18.75$, and $C_c = 19.02$. Furthermore, as $\epsilon \rightarrow 0$, the rescaled and shifted potential

$$\tilde{U}_c^*(z) \equiv U_c^*(z^* + z) / |U_{c,\min}^*| \quad (6.23)$$

TABLE I. Fixed-point parameters as a function of dimensionality d . The critical fixed-point potential, $U_c^*(z)$, attains its minimum at $z = z^*$. The abscissae z_k^0 and z_k^c are defined by $U_0^*(z_k^0) = U_c^*(z_k^c) = k \geq 0$ and then $\Delta z_{k,k'}^c = z_k^c - z_{k'}^c$, $\Delta z_{k,k'}^0 = z_k^0 - z_{k'}^0$ describe the shape of the repulsive parts of the potentials while $\Delta z_k^* = z_k^0 - z_k^c$ measures the separation between U_0^* and U_c^* . The data have been computed with rescaling factor $b=2$.

d	z^*	z_1^0	$\Delta z_{1,2}^c$	$\Delta z_{1,2}^0$	$\Delta z_{2,4}^c$	$\Delta z_{2,4}^0$	Δz_1^*	$-U_{c,\min}^*$	λ_1
2	0.714	1.51	0.02 ₆	0.23 ₀	0.04 ₀	0.22 ₁	1.148	1.975	0.49
2.8	13.09	13.59	0.28 ₄	0.36 ₀	0.31 ₃	0.37 ₇	1.91	3.64×10^{-2}	0.31
2.9	29.39	29.73	0.34 ₃	0.39 ₂	0.37 ₃	0.41 ₆	2.38	6.33×10^{-3}	0.22
2.95	62.46	62.70	0.38 ₂	0.41 ₃	0.41 ₁	0.44 ₅	3.05	8.86×10^{-4}	0.15
2.975	129.1	129.3	0.40 ₀	0.42 ₆	0.43 ₆	0.45 ₈	3.9 ₀	1.00×10^{-4}	0.10
3	∞	∞	0.44 ₄		0.47 ₃		∞	0	0

appears to approach a well-defined function near its minimum: this is illustrated in Fig. 7. It should be possible to derive (or correct!) these results by analytic studies of our recursion relation for $b > 1$ or of the differential form for $b \rightarrow 1$ but we have not yet achieved this.

C. Relevant short-range perturbations

Within the SFL regime, there is only one relevant perturbation at the critical fixed point $U_c^*(z)$. The corresponding scaling index, λ_1 , yields the exponent

$$\nu_{\parallel} = 1/\lambda_1, \quad (6.24)$$

for the divergence of the parallel correlation length ξ_{\parallel} as defined in (3.49). This exponent has been determined by studying the RG trajectories in the vicinity of $U_c^*(z)$.

Consider an initial potential $U^{(0)}(z)$ close to the critical manifold. Then, after N iterations of the RG, the potential $U^{(N)}$ is close to the fixed point $U_c^*(z)$. Typical values encountered for $b=2$ were $N \simeq 20$ for $d=2$ and $N \simeq 50$ for $d=2.95$. Then, one may expand the difference $U^{(N)} - U_c^*$ in terms of the eigenperturbations $f_i(z)$, of the linearized RG as

$$U^{(N)}(z) = U_c^*(z) + \sum_{i \geq 1} c_i^{(N)} f_i(z) \quad (6.25)$$

with coefficients $c_i^{(N)}$. The perturbation $f_i(z)$ has an eigenexponent λ_i so that

$$\bar{R}[U_c^*(z) + c_i^{(N)} f_i(z)] \approx U_c^*(z) + b^{\lambda_i} c_i^{(N)} f_i(z). \quad (6.26)$$

For initial potentials without power-law tails, the leading irrelevant scaling exponent is $\lambda_2 = -\frac{1}{2}\epsilon$, as mentioned. Thus, $\lambda_i < \lambda_2$ for $i > 2$ and further iteration of the RG leads to

$$U^{(N+M)}(z) = U_c^*(z) + E_M(z) \quad (6.27)$$

with deviation

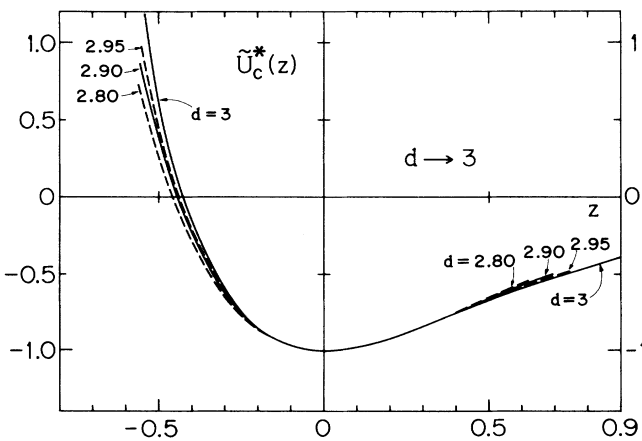


FIG. 7. The rescaled and shifted critical fixed-point potentials for dimensionalities approaching $d=3$, for which a definite limiting form appears to exist.

$$E_M(z) \approx b^{\lambda_1 M} c_1^{(N)} f_1(z) + b^{-\epsilon M/2} c_2^{(N)} f_2(z) + \dots \quad (6.28)$$

provided $b^{\lambda_1 M} c_1^{(N)} f_1 \ll 1$ which justifies the use of the linearized RG. For sufficiently large $N+M$, the irrelevant perturbations in (6.28) are numerically small, and may be neglected. It proves most convenient to use this relation at the minimum of $U^{(N+M)}(z)$ at location

$$z = z_{N+M} = z^* + O(E) \quad \text{with } E = c_1^{(N)} f_1(z^*), \quad (6.29)$$

where z^* is the location of the minimum of the fixed-point potential $U_c^*(z)$. Consequently, one has

$$U_{\min}^{(N+M)} \equiv U^{(N+M)}(z_{N+M}) = U_c^*(z^*) + b^{n\lambda_1} E + O(E^2), \quad (6.30)$$

so that the ratio

$$S_N \equiv (U_{\min}^{(N+2)} - U_{\min}^{(N+1)}) / (U_{\min}^{(N+1)} - U_{\min}^{(N)}) \quad (6.31)$$

can be employed to estimate λ_1 via

$$\lambda_1^{(N)} \equiv \ln S_N / \ln b = \lambda_1 + O(E). \quad (6.32)$$

In practice, it proves effective to change the chosen parameter in the initial potential $U^{(0)}(z)$ until $\lambda_1^{(N)}$ exhibits a plateau value as a function of N for initial potentials located on either side of the critical locus (which is a separatrix for the flows). In this way, the scaling index λ_1 has been determined for several values of d . The numerical results are collected in Table I for $b=2$. The estimate $\lambda_1 = 0.49 \pm 0.01$ found for $d=2$ is in good agreement with the exact value $\lambda_1 = \frac{1}{2}$.³⁵ It is remarkable that ν_{\parallel} increases with d : this is quite unexpected since fluctuations normally become less important as d increases leading to a decrease of ν_{\parallel} towards its mean-field value. However, we find that $\nu_{\parallel} = 1/\lambda_1$ exhibits highly singular behavior as $\epsilon = (3-d) \rightarrow 0$. An excellent fit to the data in Table I for $2 \leq d \leq 2.975$ is provided by the divergent form⁹

$$\nu_{\parallel} \simeq \epsilon^{-1/2} \left[\frac{1}{2} \ln(B/\epsilon) + C\epsilon \right]^{1/2}, \quad (6.33)$$

with $B=3$ and $C=3.65$ (for rescaling factor $b=2$). Thus, as $d \rightarrow 3^-$, we have “critical exponents for critical exponents” and, probably, logarithmic factors also. For $d=3$, $\nu_{\parallel} = \infty$ follows by continuity from (6.33). Again, it should be possible to check the form (6.33) analytically.

D. Long-range perturbations

For $d < 3$, we can readily study the effect of long-ranged perturbations at the fixed points. Thus, consider an initial potential

$$U^{(0)}(z) = U^*(z) + E^{(0)}(z), \quad (6.34)$$

which has a power-law tail of the form

$$E^{(0)}(z) \approx C_r^{(0)} / z^r \quad \text{as } z \rightarrow \infty, \quad (6.35)$$

with $C_r^{(0)}$ small. Then, the recursion relation (4.32) and the fixed-point relation (6.1) lead to $U^{(1)}(z) = U^*(z) + E^{(1)}(z)$ with

$$E^{(1)}(z) \approx b^{d-1} \exp[U^*(z)/b^{d-1}] \times \int_{-\infty}^{\infty} \frac{dy}{\sqrt{\pi}} e^{-y^2 - K^*(y,z)} E^{(0)}(b^{\zeta}z - y), \quad (6.36)$$

correct to first order in $E^{(0)}$, where

$$K^*(y,z) \equiv \frac{1}{2} U^*(b^{\zeta}z - y) + \frac{1}{2} U^*(b^{\zeta}z + y). \quad (6.37)$$

Now, we have seen that the tails of the short-ranged fixed-point potentials decay faster than exponentially and, indeed, are probably Gaussian for all b as for $b \rightarrow 1$. Therefore, the asymptotic behavior of $E^{(1)}(z)$ for large z follows from

$$E^{(1)}(z) \approx b^{d-1} \int_{-\infty}^{\infty} \frac{dy}{\sqrt{\pi}} e^{-y^2} E^{(0)}(b^{\zeta}z - y) \approx b^{d-1} \exp\left[\frac{1}{4} \frac{d^2}{dx^2}\right] E^{(0)}(x) \Big|_{x=b^{\zeta}z}. \quad (6.38)$$

Using (6.35) and writing $E^{(1)}(z)$ in the same form when $z \rightarrow \infty$ yields

$$C_r^{(1)} = b^{d-1-\zeta r} C_r^{(0)}. \quad (6.39)$$

Thus, power-law tails in the potential represent perturbations with a scaling exponent

$$\lambda_r = d - 1 - \zeta r = (\tau - r)\zeta \quad (6.40)$$

[where $\tau = 2(d-1)/(3-d)$ as before]. It is interesting to note that the same result follows simply by rescaling the potential $E^{(0)}(z)$ according to (4.3) and (4.4) with $z \propto l$. Now, provided $r > \tau$, so that the power-law tail decays sufficiently rapidly, the initial potential (6.34) belongs to the SFL regime in accord with (3.51); these perturbations are then *irrelevant*. Thus, for $r > \tau$, one has *universal* critical behavior with $\nu_{\parallel} = 1/\lambda_1$ and λ_1 determined from the fixed point U_c^* .

For $r = \tau$, the long-ranged perturbations become *marginal*. In this case, nonuniversal behavior is to be expected as has been shown explicitly for $d=2$, when $r = \tau(d=2) = 2$, by transfer-matrix methods.³⁰ This behavior is presumably governed by a line of nontrivial fixed points with $U^*(z) \sim 1/z^{\tau}$ for large z but we have not investigated this point for general $d < 3$.

Finally, let us consider perturbations of the form

$$E^{(0)}(z) \approx -C_r^{(0)}/z^r + C_s^{(0)}/z^s, \quad (6.41)$$

with $C_r^{(0)}$ and $C_s^{(0)}$ both small and positive: compare with (2.4). Then, the attractive part is governed by the scaling exponent (6.40) while the repulsive part likewise has scaling index $\lambda_s = d - 1 - \zeta s = (\tau - s)\zeta$. If $r < \tau < s$, the attractive part is relevant and the repulsive part is irrelevant: in that case, we obtain

$$\nu_{\parallel} = 1/\lambda_r, \quad (6.42)$$

which is just the result (3.50) for the weak-fluctuation regime. On the other hand, if $r < s < \tau$, both parts of the potential are relevant and grow under the RG. This is the regime governed by mean-field theory and all exponents are readily found by minimization of the total potential.

VII. DISCUSSION AND OUTLOOK

We have studied the unbinding (or depinning or delocalization) of interfaces subject only to thermal fluctuations. A simple picture was presented in Sec. III in which the direct interaction between the interfaces arising from molecular forces is compared with steric interactions induced by interfacial fluctuations; see Sec. III C. This picture clarifies the origin and nature of the various scaling regimes for critical (and, also, for multicritical) unbinding or wetting transitions. In addition, it gives quantitatively correct results for the critical behavior in both the MF and WFL regimes.

An approximate functional renormalization group, which acts on the potentials, $V(l)$, of interaction between interfaces, was introduced in Sec. IV and analyzed for arbitrary rescaling factor $b > 1$. The corresponding relations are exact to first order in V . In the infinitesimal rescaling limit, the functional RG leads to the simple but nonlinear flow equation (4.14) for the potential $V(l)$. The bounds derived in Sec. V show that the nonlinearities (which allow for infinite or ‘‘hard wall’’ potentials) have relatively weak effects. Nevertheless, the nonlinearities lead, as shown in Sec. VI, to the existence of two nontrivial fixed-point potentials, $V_0^*(l) \propto U_0^*(z)$ and $V_c^*(l) \propto U_c^*(z)$, in the SFL regime when $d < d_0 = 3$. On approach to $d = 3$ these fixed points do *not* coalesce with the standard trivial Gaussian fixed point in the typical bifurcation scenario; rather, they mutually annihilate leaving behind a line of novel ‘‘drifting’’ fixed points;⁹ see Fig. 7. The fixed-point potential $V_0^*(l)$ describes the completely delocalized phase of the interfaces. At this fixed point, all perturbations lying within the SFL regime which, by definition, thus satisfy (3.51), are irrelevant. The fixed point $V_c^*(l)$, on the other hand, governs the manifold of critical unbinding transitions: at $V_c^*(l)$, there is one relevant perturbation within the SFL regime; see Sec. VI C.

The results obtained from the functional RG have the following important consequences.

- (i) The unusual bifurcation in $d = d_0 = 3$ explains why standard perturbation schemes analogous to the ϵ expansion for bulk critical phenomena³⁶ are not directly applicable.
- (ii) The existence of the fixed point $V_c^*(l)$ with associated critical manifold of codimension one, leads to *universal* critical behavior within the SFL regime.
- (iii) The study of short- and long-range perturbations at $V_0^*(l)$ leads to a unified description of all three scaling regimes.

- (iv) Reliable estimates for the values of the critical exponents ν_{\parallel} , etc., in the SFL regime for $d < d_0$ can be obtained by numerically iterating the recursion relations for $V(l)$.

As an alternative to the numerical techniques presented in Sec. VI, it would be useful to develop a more analytical approach. In particular, it seems possible to make some progress, on the basis of the differential flow equation (4.14). This equation is nontrivial because of the nonlinearities in combination with the rescaling term $\zeta l (\partial V / \partial l)$, which represents a singular perturbation near $d = 3$ ($\zeta = 0$).

A more analytical approach should, in particular, help

the study of two topics which are difficult to handle by direct numerical techniques; namely: (i) the critical behavior for $d=d_2(r)$ as governed by (3.47), i.e., on the *boundary* between the WFL and the SFL regimes. Here, nonuniversal behavior, presumably governed by a line of nontrivial fixed points, is to be expected as has been found explicitly^{6,30} when $d=d_2(r=2)=2$. In addition, (ii) *tricritical behavior* for $d_0=3>d>2$, which should be governed by a new nontrivial fixed point potential, say, $V_t^*(l)$, which is expected to exhibit a maximum at large l and a minimum at small l .

The renormalization-group approach introduced here has also been applied to the unbinding of tensionless membranes.^{37,5} In this case, the boundary dimension is $d_u=5$, which means that universal critical behavior, governed by a nontrivial fixed point V_c^* , can be found in realistic three-dimensional systems subject to long-range power-law interactions.³⁷ Finally, the simple picture for

distinguishing scaling regimes has also been used to study the unbinding of interfaces in the presence of *random* potentials which arise, e.g., from quenched impurities.^{8,4} It would be most interesting to generalize the functional RG described here to such cases so as to study the analogous strong fluctuation regimes.

ACKNOWLEDGMENTS

The interest and comments of Daniel S. Fisher, David A. Huse, Daniel M. Kroll, and Stanislas Leibler have been much appreciated. Our work has been supported by the National Science Foundation, principally through the Condensed Matter Theory Program,³⁸ but in part through the Materials Science Center at Cornell University. We are also grateful for the hospitality of the Aspen Center for Physics where part of this manuscript was written.

*Present address: Institut für Festkörperforschung, KFA Jülich, Postfach 1913, 5170 Jülich, West Germany.

¹For a review of roughening transitions see; J. D. Weeks, in *Ordering in Strongly Fluctuating Condensed Matter Systems*, edited by T. Riste (Plenum, New York 1980).

²A review of wetting phenomena is provided by D. E. Sullivan and M. M. Telo da Gama in *Fluid Interfacial Phenomena*, edited by C. A. Croxton (Wiley, New York, 1985), p. 45. Wetting in the context of adsorption is discussed in R. Pandit, M. Schick, and M. Wortis, *Phys. Rev. B* **26**, 5112 (1982).

³Complete wetting phenomena are considered by R. Lipowsky, *Phys. Rev. B* **32**, 1731 (1985).

⁴A review of wetting and commensurate-incommensurate transitions in homogeneous and random media is provided by M. E. Fisher, *J. Chem. Soc. Faraday Trans. 2*, **82**, 1569 (1986).

⁵See, e.g., S. Leibler and R. Lipowsky, *Phys. Rev. B* **35**, 7004 (1987).

⁶D. M. Kroll, R. Lipowsky, and R. K. P. Zia, *Phys. Rev. B* **32**, 1862 (1985).

⁷D. S. Fisher and D. A. Huse, *Phys. Rev. B* **32**, 247 (1985).

⁸R. Lipowsky and M. E. Fisher, *Phys. Rev. Lett.* **56**, 472 (1986).

⁹R. Lipowsky and M. E. Fisher, *Phys. Rev. Lett.* **57**, 2411 (1986).

¹⁰K. G. Wilson, *Phys. Rev. B* **4**, 3184 (1971); K. G. Wilson and M. E. Fisher, *Phys. Rev. Lett.* **28**, 240 (1972).

¹¹A. M. Szpilka and M. E. Fisher, *Phys. Rev. Lett.* **57**, 1044 (1986).

¹²M. E. Fisher, *J. Stat. Phys.* **34**, 667 (1984).

¹³W. Selke, D. A. Huse, and D. M. Kroll, *J. Phys. A* **17**, 3019 (1984).

¹⁴C. Herring, in *Structure and Properties of Solid Surfaces*, edited by R. Gomer and C. S. Smith (University of Chicago Press, Chicago, 1953).

¹⁵M. E. Fisher and D. S. Fisher, *Phys. Rev. B* **25**, 3192 (1982).

¹⁶M. P. A. Fisher, D. S. Fisher, and J. D. Weeks, *Phys. Rev. Lett.* **48**, 368 (1982).

¹⁷R. Lipowsky, D. M. Kroll, and R. K. P. Zia, *Phys. Rev. B* **27**, 4499 (1983); R. Lipowsky, *J. Appl. Phys.* **55**, 2485 (1984).

¹⁸E. Brézin, B. I. Halperin, and S. Leibler, *Phys. Rev. Lett.* **50**,

1387 (1983).

¹⁹T. Aukrust and E. H. Hauge, *Phys. Rev. Lett.* **54**, 1814 (1985), and, especially, E. H. Hauge and K. Olaussen, *Phys. Rev. B* **32**, 4766 (1985).

²⁰R. Lipowsky and D. M. Kroll, *Phys. Rev. Lett.* **52**, 2303 (1984).

²¹D. M. Kroll and T. Meister, *Phys. Rev. B* **31**, 6134 (1985).

²²M. P. Nightingale, W. F. Saam, and M. Schick, *Phys. Rev. B* **30**, 3830 (1984).

²³S. Dietrich and M. Schick, *Phys. Rev. B* **31**, 4718 (1985).

²⁴C. Ebner, W. F. Saam, and A. K. Sen, *Phys. Rev. B* **31**, 6134 (1985).

²⁵P. G. de Gennes, *C. R. Acad. Sci. Paris* **297**, 9 (1983).

²⁶R. Lipowsky, *Phys. Rev. Lett.* **52**, 1429 (1984).

²⁷See, e.g., J. N. Israelachvili, *Intermolecular and Surface Forces* (Academic, London, 1985).

²⁸R. Lipowsky, *Z. Phys. B* **55**, 335 (1984).

²⁹D. B. Abraham, *Phys. Rev. Lett.* **44**, 1165 (1980).

³⁰D. M. Kroll and R. Lipowsky, *Phys. Rev. B* **28**, 5273 (1983).

³¹K. G. Wilson (unpublished) has recently constructed a complete orthonormal set of functions which are exponentially localized both in real space and in momentum space.

³²A pedagogical description of Wilson's approximate recursion relations is presented in S.-K. Ma, *Modern Theory of Critical Phenomena* (Benjamin, Reading, Mass., 1976).

³³A. Hasenfratz and P. Hasenfratz, *Nucl. Phys. B* **270** [FS16] 687 (1986).

³⁴See, e.g., M. E. Fisher, *J. Math. Phys.* **6**, 1643 (1965).

³⁵Following from D. B. Abraham's exact solution [*Phys. Rev. Lett.* **44**, 1165 (1980)] for a $d=2$ Ising model. This yields a specific-heat exponent $\alpha=0$ and a layer thickness exponent $\psi \equiv -\beta_s = 1$. The scaling relations $(2-\alpha)=(d-1)\nu_{\parallel}$, $\nu_{\perp} = \psi = \zeta\nu_{\parallel}$ with $\zeta = \frac{1}{2}(3-d)$ for $d \leq 3$ may then be used; see Refs. 2, 4, and 6.

³⁶See, e.g., M. E. Fisher, in *Critical Phenomena*, edited by F. J. W. Hahne, Vol. 186 of *Lecture Notes in Physics* (Springer-Verlag, Berlin, 1983), p. 1.

³⁷R. Lipowsky and S. Leibler, *Phys. Rev. Lett.* **56**, 2541 (1986).

³⁸Through Grant No. DMR 81-17011.